Dynamics of PDE, Vol.x, No.y, xx-yy, 2008

Location and phase segregation of ground and excited states for 2D Gross–Pitaevskii systems

Marco Caliari and Marco Squassina

Communicated by Charles Li, received December 4, 2007 and, in revised form, February 20, 2008.

Abstract. We consider a system of Gross–Pitaevskii equations in $\mathbb{R}^2$ modelling a mixture of two Bose–Einstein condensates with repulsive interaction. We aim to study the qualitative behaviour of ground and excited state solutions. We allow two different harmonic and off-centered trapping potentials and study the spatial patterns of the solutions within the Thomas–Fermi approximation as well as phase segregation phenomena within the large-interaction regime.

Contents

1. Introduction

The first successful experimental realization of Bose–Einstein condensates for atomic gases [**4**], which goes back to 1995, gave rise to various numerical and theoretical investigations on the macroscopic equation ruling these phenomena,

2000 *Mathematics Subject Classification.* Primary 35B40, 35Q55; Secondary 81V05, 81V45.
Key words and phrases. Gross–Pitaevskii equations, Bose–Einstein binary condensates, ground states, location of solutions, phase-segregation of solutions.
The research of the second author was partially supported by the MIUR national research project *Variational and Topological Methods in the Study of Nonlinear Phenomena*.

that is the Gross–Pitaevskii equation (GPE)

$$\hbar i\partial_t\psi = -\frac{\hbar^2}{2m}\Delta\psi + V(x)\psi + \vartheta|\psi|^2\psi, \quad x \in \mathbb{R}^n, \quad \vartheta \geq 0.$$

More recently, in 1997, Bose–Einstein condensation for a mixture of two different interacting atomic species with the same mass was firstly realized at JILA [**26**] exhibiting a partial overlap between the wave functions. The vector nature of the order parameter gives rise to some intriguing structures and dynamics that are absent in the single component case. This, again, stimulated various succeeding studies of numerical and theoretical nature. For both single or binary condensates we refer the reader to [**13**,**30**] and to the references therein. Recently, some efficient numerical techniques have been developed to compute ground state solutions of GPE [**6**, **9**], which can be used to investigate the vector case. On this basis, in this paper we deal with the rigorous analysis of the spatial configurations for the standing wave solutions (ground and excited states) of the system in $\mathbb{R}^2$

$$\begin{cases} \hbar i\partial_t\psi_1 = -\frac{\hbar^2}{2m_1}\Delta\psi_1 + V_1(x_1,x_2)\psi_1 + \vartheta_{11}\hbar^2|\psi_1|^2\psi_1 + \vartheta_{12}\hbar^2|\psi_2|^2\psi_1, \\ \hbar i\partial_t\psi_2 = -\frac{\hbar^2}{2m_2}\Delta\psi_2 + V_2(x_1,x_2)\psi_2 + \vartheta_{21}\hbar^2|\psi_1|^2\psi_2 + \vartheta_{22}\hbar^2|\psi_2|^2\psi_2, \end{cases} \tag{1.1}$$

for the unknown $\psi_i : \mathbb{R}^2 \to \mathbb{C}$, $i = 1, 2$, where $\hbar$ denotes the (reduced) Planck constant and the coefficients $\vartheta_{ij} \geq 0$ (defocusing case), with $\vartheta_{12} = \vartheta_{21}$, are given by the formula [**15**]

$$\vartheta_{ij} = 2\pi\sigma_{ij}\frac{m_i + m_j}{m_i m_j}, \quad \sigma_{ij} = \sigma_{ji}, \quad i, j = 1, 2,$$

being σ_{ij} related to the scattering lengths and m_i the atomic masses of the two species composing the mixture. Considering the 2D case is not restrictive as there are various situations where the full 3D system can be reduced to a 2D system with suitably modified coefficients (see e.g. Section 2.2 of [**5**]). The coefficients ϑ_{ii} and ϑ_{12} play the role of repulsive intra-species and inter-species parameters respectively. As we will see, when ϑ_{12} is sufficiently large, then some interesting overlap and spatial segregation phenomena between the wave densities occur. Concerning the potentials, we let $V_i(x_1, x_2) = \frac{m_i}{2}(\omega_{i1}^2(x_1 - x_{i1})^2 + \omega_{i2}^2(x_2 - x_{i2})^2)$ for (x_1, x_2) in $\mathbb{R}^2$, where $\omega_{ij} > 0$, $i, j = 1, 2$. A typical situation is when the V_is have the same center, without loss of generality, the origin. On the other hand, there are some physical situations reported in literature, which lead to consider off-centered potentials. See, for instance, [**32**], where the vertical direction in the potential is not aligned with the symmetry axis of the trap. Similar equations have also arisen as governing equations for electromagnetic pulse propagation in "left-handed" materials with Kerr-type nonlinearity [**19**], in the modified Hubbard model in the long-wavelength approximation [**22**,**23**], in quadratic nonlinear materials with suitable phase matching [**18**] and in nonlinear optics, for instance in the propagation of pulses in a nonlinear optical fiber of bi-modal type due to the presence of some birefringence effects generating two pulses with different polarization directions [**24**]. For a wide discussion on nonlinear Schrödinger systems we refer the interested reader to [**1**–**3**] and to the references therein.

Let $\mathcal{H}$ be the Hilbert subspace of $H^1(\mathbb{R}^2, \mathbb{C}) \times H^1(\mathbb{R}^2, \mathbb{C})$ defined by

$$\mathcal{H} = \left\{ (\psi_1, \psi_2) \in H^1(\mathbb{R}^2, \mathbb{C}) \times H^1(\mathbb{R}^2, \mathbb{C}) : \int_{\mathbb{R}^2} V_i(x_1, x_2)|\psi_i|^2 < \infty, \ i = 1, 2 \right\},$$

which is the natural framework for bound state solutions, endowed with the norm

$$\|(\psi_1,\psi_2)\|^2_{\mathcal{H}} = \sum_{i=1}^{2} \frac{\hbar^2}{2m_i}\int_{\mathbb{R}^2} |\nabla\psi_i|^2 + \int_{\mathbb{R}^2} V_i(x_1,x_2)|\psi_i|^2,$$

and consider the total energy functional $E : \mathcal{H} \to \mathbb{R}$ associated with (1.1)

$$E(\psi_1(\cdot,t),\psi_2(\cdot,t)) = \sum_{i=1}^{2} E_i(\psi_i(\cdot,t)) + \vartheta_{12}\hbar^2 \int_{\mathbb{R}^2} |\psi_1(\cdot,t)|^2|\psi_2(\cdot,t)|^2, \tag{1.2}$$

where, for $i = 1, 2$, we set

$$E_i(\psi_i(\cdot,t)) = \frac{\hbar^2}{2m_i}\int_{\mathbb{R}^2} |\nabla\psi_i(\cdot,t)|^2 + \int_{\mathbb{R}^2} V_i(x_1,x_2)|\psi_i(\cdot,t)|^2 + \frac{\vartheta_{ii}\hbar^2}{2}\int_{\mathbb{R}^2} |\psi_i(\cdot,t)|^4.$$

By multiplying the first equation of system (1.1) by $\partial_t\bar{\psi}_1$ and the second by $\partial_t\bar{\psi}_2$, taking the real parts, integrating and adding the resulting identities, it is readily seen that E is constant on the solutions, namely $E(\psi_1(\cdot,t),\psi_2(\cdot,t)) = E(\psi_1(\cdot,0),\psi_2(\cdot,0))$ for any $t \geq 0$. Also, as for the case of the single equation, by multiplying the first equation of (1.1) by $\bar{\psi}_1$ and the second by $\bar{\psi}_2$, taking the imaginary parts, integrating and adding the resulting identities, it turns out that the total number of particles N_i of the i-th species is time independent (preservation of the particle number), namely

$$\int_{\mathbb{R}^2} |\psi_i(\cdot,t)|^2 = N_i, \qquad t \geq 0,\ i = 1,2. \tag{1.3}$$

The *ground state* (or least energy) solution of (1.1) is a solution with ansatz

$$\psi_i(x_1,x_2,t) = e^{-\mathrm{i}\frac{\mu_i t}{\hbar}}\phi_i(x_1,x_2), \qquad (x_1,x_2) \in \mathbb{R}^2,\ t \geq 0,\ \ i = 1,2, \tag{1.4}$$

where the pair (ϕ_1,ϕ_2) is real valued and minimizes functional (1.2) constrained to conditions (1.3) (with ϕ_i in place of ψ_i). As a consequence, the ϕ_is solve the nonlinear eigenvalue problem in $\mathbb{R}^2$

$$\begin{cases} -\frac{\hbar^2}{2m_1}\Delta\phi_1 + V_1(x_1,x_2)\phi_1 + \vartheta_{11}\hbar^2|\phi_1|^2\phi_1 + \vartheta_{12}\hbar^2|\phi_2|^2\phi_1 = \mu_1\phi_1, \\ -\frac{\hbar^2}{2m_2}\Delta\phi_2 + V_2(x_1,x_2)\phi_2 + \vartheta_{21}\hbar^2|\phi_1|^2\phi_2 + \vartheta_{22}\hbar^2|\phi_2|^2\phi_2 = \mu_2\phi_2, \\ \displaystyle\int_{\mathbb{R}^2}\phi_1^2 = N_1,\ \ \int_{\mathbb{R}^2}\phi_2^2 = N_2. \end{cases} \tag{1.5}$$

Testing the first equation of (1.5) by $\bar{\psi}_1$ and the second by $\bar{\psi}_2$, we have a formula for the eigenvalues μ_i (also known as chemical potentials) versus the eigenvectors ϕ_i

$$N_i\mu_i = E_i(\phi_i) + \frac{\vartheta_{ii}}{2}\hbar^2\int_{\mathbb{R}^2}|\phi_i|^4 + \vartheta_{12}\hbar^2\int_{\mathbb{R}^2}|\phi_1|^2|\phi_2|^2, \qquad i = 1,2. \tag{1.6}$$

The existence of ground state solutions to (1.1) in $\mathcal{H}$ is reduced to the existence of minima for the energy functional (1.2) constrained to

$$\mathcal{S} = \{(\phi_1,\phi_2) \in \mathcal{H} :\ \|\phi_i\|^2_{L^2} = N_i,\ i = 1,2\}. \tag{1.7}$$

As the ϑ_{ij} are positive,

$$\frac{\vartheta_{11}}{2}|\phi_1|^4 + \vartheta_{12}|\phi_1|^2|\phi_2|^2 + \frac{\vartheta_{22}}{2}|\phi_2|^4 \geq 0,$$

so that the energy functional E is coercive, bounded from below and weakly lower semi-continuous over $\mathcal{S}$. Hence, the existence of a ground state solution is immediately guaranteed. Usually, with reference to the solutions of the form (1.4) (standing waves), there are two possible (physically different) approaches depending on whether one considers the chemical potentials μ_i as fixed (hence searching for solutions to the first two equations in (1.5) but with possibly different L^2 norms) or the total masses $\int_{\mathbb{R}^2} |\phi_i|^2$ as fixed (thus solving the nonlinear eigenvalue problem (1.5), which is the case we deal with). Any other solution (ϕ_1, ϕ_2) of system (1.5) of the form (1.4) not having minimal energy for E will be called *excited state* (or higher energy solution).

The main goal of this paper is to prove some geometrical properties (clearly confirmed by some numerical simulations) for ground and excited state of (1.5), particularly under the influence of strong interaction effects (namely $\vartheta_{12} \to \infty$). See e.g. Propositions 3.1 and 3.2.

In Section 2 we derive the location of ground state solutions via the Thomas–Fermi approximation and classify the relative configuration of ϕ_i with respect to ϕ_j. In Section 3 we study the phase separation process (spatial segregation) in the large competition regime. In Section 4, for the sake of completeness, we briefly describe the functional framework of the numerical scheme used to compute the solutions.

In the following the Hilbert space $L^2(\mathbb{R}^2, \mathbb{C})$ is endowed with the standard scalar product $(f, g)_2 = \int_{\mathbb{R}^2} f\bar{g}$, for $f, g \in L^2(\mathbb{R}^2)$, and the induced is denoted by $\|\cdot\|_{L^2}$.

2. Location and Thomas–Fermi approximation

If the distance between the centers of the trapping potentials V_i is sufficiently small compared with the radii of the supports of the ground state solutions ϕ_i, then the condensates share a region where they coexist (with a partial or full overlap, that is one condensate is partially or entirely included in the other). In the opposite case the supports of the wave functions are disjoint. Hence, we can encounter three different patterns for the spatial wave functions ϕ_i, which we are going to discuss, namely: *no* overlap, *partial* overlap and *full* overlap. It should be noted that *support* just means here the planar region where the mass of the ground state solution is mainly concentrated, being (exponentially) vanishing on the outside. In the Thomas–Fermi regime, an approximation of the ground state solutions of system (1.5), which is very good for sufficiently large values of the coupling constants, can be obtained by simply dropping the diffusion terms $-\Delta\phi_i$, namely the kinetic contributions, thus assuming the wave functions to be slowly varying (cf. [**16**, **20**, **21**, **35**]). In turn, (1.5) reduces to the algebraic system (here we let $\hbar = 1$)

$$\begin{cases} 2\vartheta_{11}|\phi_1|^2 + 2\vartheta_{12}|\phi_2|^2 = 2\mu_1 - (x_1 - x_{11})^2 - (x_2 - x_{12})^2, \\ 2\vartheta_{21}|\phi_1|^2 + 2\vartheta_{22}|\phi_2|^2 = 2\mu_2 - (x_1 - x_{21})^2 - (x_2 - x_{22})^2, \end{cases} \tag{2.1}$$

where the μ_is should be computed through the normalization conditions (1.3) (if, for instance, $\vartheta_{12} = 0$, it holds $\mu_i \propto \sqrt{\vartheta_{ii}}$ for $i = 1, 2$). In general, as the left-hand sides are positive, this system is satisfied only on a (possibly empty) subset $\mathcal{O} \subset \mathbb{R}^2$ ($\mathcal{O} = \mathcal{O}_1 \cap \mathcal{O}_2$ in the notations introduced below), namely the overlap region. It is natural to introduce the circumferences defined by $(x_1 - x_{i1})^2 + (x_2 - x_{i2})^2 = r_i^2$, with

$r_i(\mu_i) = \sqrt{2\mu_i}$, $i = 1, 2$. The intersection of the corresponding disks $\mathcal{D}_i$ gives the region where system (2.1) makes sense. Outside the region $\mathcal{O}$, the wave functions take the usual form of the solutions of the GPE ($\vartheta_{12} = 0$) in the Thomas–Fermi regime (see the expressions below of ϕ_i on $\mathcal{D}_i \setminus \mathcal{O}$). More precisely, we have the following non-smooth approximations of the ground state (see also the work by Riboli and Modugno [**32**])

$$\phi_1 = \begin{cases} \sqrt{\frac{\vartheta_{22}(2\mu_1-(x_1-x_{11})^2-(x_2-x_{12})^2)-\vartheta_{12}(2\mu_2-(x_1-x_{21})^2-(x_2-x_{22})^2)}{2(\vartheta_{11}\vartheta_{22}-\vartheta_{12}^2)}}, & \text{in } \mathcal{O}, \\ \sqrt{\frac{2\mu_1-(x_1-x_{11})^2-(x_2-x_{12})^2}{2\vartheta_{11}}}, & \text{in } \mathcal{D}_1 \setminus \mathcal{O}, \\ 0, & \text{in } \mathbb{R}^2 \setminus \mathcal{D}_1, \end{cases}$$

$$\phi_2 = \begin{cases} \sqrt{\frac{\vartheta_{11}(2\mu_2-(x_1-x_{21})^2-(x_2-x_{22})^2)-\vartheta_{12}(2\mu_1-(x_1-x_{11})^2-(x_2-x_{12})^2)}{2(\vartheta_{11}\vartheta_{22}-\vartheta_{12}^2)}}, & \text{in } \mathcal{O}, \\ \sqrt{\frac{2\mu_2-(x_1-x_{21})^2-(x_2-x_{22})^2}{2\vartheta_{22}}}, & \text{in } \mathcal{D}_2 \setminus \mathcal{O}, \\ 0, & \text{in } \mathbb{R}^2 \setminus \mathcal{D}_2, \end{cases}$$

that is, equivalently,

$$\phi_i = \begin{cases} \sqrt{\alpha_i(R_i^2 - (x_1 - y_{i1})^2 - (x_2 - y_{i2})^2)}, & \text{in } \mathcal{O}, \\ \sqrt{\frac{r_i^2-(x_1-x_{i1})^2-(x_2-x_{i2})^2}{2\vartheta_{ii}}}, & \text{in } \mathcal{D}_i \setminus \mathcal{O}, \\ 0, & \text{in } \mathbb{R}^2 \setminus \mathcal{D}_i, \end{cases} \tag{2.2}$$

where, according to the notations introduced below, $\mathcal{O} = \mathcal{O}_1 \cap \mathcal{O}_2$, $\mathcal{D} = \mathcal{D}_1 \cap \mathcal{D}_2$,

$$\mathcal{O}_i = \big\{(x_1, x_2) \in \mathcal{D} : \ (x_1 - y_{i1})^2 + (x_2 - y_{i2})^2 \leq (\geq) R_i^2\big\},$$
$$\mathcal{D}_i = \big\{(x_1, x_2) \in \mathbb{R}^2 : \ (x_1 - x_{i1})^2 + (x_2 - x_{i2})^2 \leq r_i^2\big\},$$

with $\leq$ (resp. $\geq$) in the definition of $\mathcal{O}_i$ for $\alpha_i > 0$ (resp. $\alpha_i < 0$), if we set

$$y_{11} = \frac{\omega_{22}x_{11} - \omega_{12}x_{21}}{\omega_{22} - \omega_{12}} = x_{11} + \frac{\omega_{12}}{\alpha_1}\Delta_1 x, \quad y_{12} = \frac{\omega_{22}x_{12} - \omega_{12}x_{22}}{\omega_{22} - \omega_{12}} = x_{12} + \frac{\omega_{12}}{\alpha_1}\Delta_2 x,$$

$$y_{21} = \frac{\omega_{11}x_{21} - \omega_{12}x_{11}}{\omega_{11} - \omega_{12}} = x_{21} - \frac{\omega_{12}}{\alpha_2}\Delta_1 x, \quad y_{22} = \frac{\omega_{11}x_{22} - \omega_{12}x_{12}}{\omega_{11} - \omega_{12}} = x_{22} - \frac{\omega_{12}}{\alpha_2}\Delta_2 x,$$

where $\Delta_j x = x_{1j} - x_{2j}$, namely, for $i, j = 1, 2$ with $i \neq j$,

$$y_{ij} = x_{ij} - (-1)^i \frac{\omega_{12}}{\alpha_i}\Delta_j x,$$

with $\omega_{ij} = \frac{\vartheta_{ij}}{2\det\Theta}$, $i, j = 1, 2$, $\alpha_1 = \omega_{22} - \omega_{12}$, $\alpha_2 = \omega_{11} - \omega_{12}$, and

$$R_1^2 = \frac{2\omega_{22}\mu_1 - 2\omega_{12}\mu_2 + \omega_{12}x_{21}^2 + \omega_{12}x_{22}^2 - \omega_{22}x_{11}^2 - \omega_{22}x_{12}^2}{\omega_{22} - \omega_{12}} + y_{11}^2 + y_{12}^2$$

$$R_2^2 = \frac{2\omega_{11}\mu_2 - 2\omega_{12}\mu_1 + \omega_{12}x_{11}^2 + \omega_{12}x_{12}^2 - \omega_{11}x_{21}^2 - \omega_{11}x_{22}^2}{\omega_{11} - \omega_{12}} + y_{22}^2 + y_{21}^2.$$

Setting $\mathbf{x_i} = (x_{i1}, x_{i2})$ and $\mathbf{y_i} = (y_{i1}, y_{i2})$ for $i = 1, 2$, this reads as

$$R_i = \sqrt{r_i^2 + \frac{2\omega_{12}}{\alpha_i}(\mu_i - \mu_j) + \frac{\omega_{12}}{\alpha_i}(|\mathbf{x_j}|^2 - |\mathbf{y_i}|^2) - \frac{\omega_{jj}}{\alpha_i}(|\mathbf{x_i}|^2 - |\mathbf{y_i}|^2)}.$$

Hence, we have four circumferences that rule the geometry of the ground states

$$\Sigma_i^r : (x_1 - x_{i1})^2 + (x_2 - x_{i2})^2 = r_i^2, \qquad \Sigma_i^R : (x_1 - y_{i1})^2 + (x_2 - y_{i2})^2 = R_i^2.$$

If $\vartheta_{12} = 0$ (namely no interaction), we deduce that $\mathbf{x_i} = \mathbf{y_i}$, $R_i = r_i$, and $\mathcal{O}_i = \mathcal{D}_i$ ($\vartheta_{12} = 0$ implies $\alpha_i > 0$), so that the ground state solutions turn into the usual Thomas–Fermi representation for the single GPE

$$\phi_i = \begin{cases} \sqrt{\frac{r_i^2 - (x_1 - x_{i1})^2 - (x_2 - x_{i2})^2}{2\vartheta_{ii}}}, & \text{in } \mathcal{D}_i, \\ 0, & \text{in } \mathbb{R}^2 \setminus \mathcal{D}_i. \end{cases}$$

If $\vartheta_{12} \approx 0$, then $\omega_{11} \approx \frac{1}{2\vartheta_{22}}$, $\omega_{22} \approx \frac{1}{2\vartheta_{11}}$, $\omega_{12} \approx 0$, $\alpha_i \approx \frac{1}{2\vartheta_{ii}}$ and $y_{ij} \approx x_{ij}$, $R_i \approx r_i$ for $i, j = 1, 2$, so that $\Sigma_i^R \approx \Sigma_i^r$ for $i = 1, 2$. If $\mathbf{x_1} = \mathbf{x_2}$, the Σ_i^Rs have centers $\mathbf{y_i} = \mathbf{x_i}$ but different radii $R_i^2 = r_i^2 + \frac{2\omega_{12}}{\alpha_i}(\mu_i - \mu_j)$, for any $i \neq j$.

2.1. Nonoverlap case. In the case occurring when the constant ϑ_{12} is zero (absence of interaction in the mixture), the system uncouples into a pair of GPEs (for the single GPE various accurate and efficient numerical techniques have been recently compared in [**9**]). Numerical experiments show that the ground state solution ϕ_i always locates its mass around the minimum point $\mathbf{x_i} = (x_{i1}, x_{i2})$ of V_i, for $i = 1, 2$. It looks apparent that boosting up the parameter ϑ_{ii} in front of the cubic nonlinearity in the equation of ϕ_i has the effect of squeezing down the profile of ϕ_i making it flatter and larger. Going back to the case $\vartheta_{12} \neq 0$, we say that we have *no overlap* between ϕ_1 and ϕ_2, if the centers $\mathbf{x_1}$ and $\mathbf{x_2}$ of Σ_i^r satisfy the geometric condition

$$(\Delta_1 x)^2 + (\Delta_2 x)^2 > |\sqrt{2\mu_1} + \sqrt{2\mu_2}|^2, \tag{2.3}$$

namely if $\mathbf{x_1}$ is sufficiently far from $\mathbf{x_2}$ with respect to the amplitudes r_i of the supports of ϕ_i. In this situation the ground state solutions look like those of the decoupled case. In fact, the coupling terms $C_{ij} = \vartheta_{12}|\phi_j|^2\phi_i$ with $i \neq j$ are almost everywhere zero as the supports are disjoint, due to (2.3). Hence the system is actually a small deformation of a pair of uncoupled GPEs. See Figure 1.

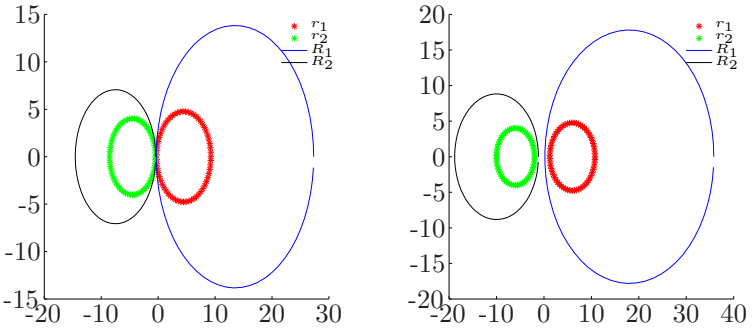

FIGURE 1. Supports of ϕ_1 and ϕ_2 (starred) and disks (unstarred) related to the Thomas–Fermi approximation for ϕ_1 and ϕ_2. We have taken $N_1 = N_2 = m_1 = m_2 = 1$, $\vartheta_{11} = 400$, $\vartheta_{22} = 200$, $\vartheta_{12} = 100$, $x_{11} = 4.5$, $x_{21} = -4.5$ (left figure, tangential supports); and $x_{11} = 6$, $x_{21} = -6$ (right figure, disjoint supports), with $x_{ij} = 0$ for any other i, j.

2.2. Partial overlap case. We have *partial overlap* between ϕ_1 and ϕ_2, if

$$|\sqrt{2\mu_1} - \sqrt{2\mu_2}|^2 < (\Delta_1 x)^2 + (\Delta_2 x)^2 < |\sqrt{2\mu_1} + \sqrt{2\mu_2}|^2,$$

namely the disks of boundaries Σ_1^r and Σ_2^r overlap without being one completely embedded in the other. We see in the contour plot of Figure 5 the partial overlap in the case $\vartheta_{11} \gg \vartheta_{22}$. Apparently, boosting ϑ_{11} with respect to ϑ_{22} makes the overlap region more localized. Keeping in mind the behaviour of the uncoupled case, in order to give this fact a very simple empirical explanation, it suffices to argue on the coupling terms C_{ij}. In the region (depending upon the relative magnitude of the ϑ_{ii}s) where both ϕ_i are nonzero the contribution of C_{ij} pushes down the profile around the origin (the center of trapping for ϕ_2), provided that ϑ_{12} is significantly large. The support of ϕ_1 still remains contractible, but the radial symmetry property of ϕ_1 is broken (due to strong interaction). See e.g. the situations reported in Figures 2 and 5. As Figure 4 shows, while the Thomas–Fermi approximation disks Σ_i^R are overlapped to the support disks Σ_i^r when the coupling constant ϑ_{12} is much smaller than the ϑ_{ii}s, in the case where $\vartheta_{12} \gg \vartheta_{ii}$, i.e. in the large interaction regime, the four circumferences intersect in two points and Σ_i^r and Σ_i^R may have quite different sizes.

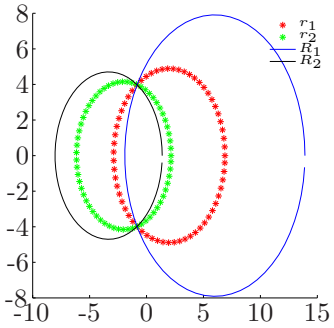

FIGURE 2. Supports of ϕ_1 and ϕ_2 (starred) and disks (unstarred) related to the Thomas–Fermi approximation for ϕ_1 and ϕ_2 (partial overlap case). We have $N_1 = N_2 = m_1 = m_2 = 1$, $\vartheta_{11} = 400$, $\vartheta_{22} = 200$, $\vartheta_{12} = 100$, $x_{11} = 2$, $x_{21} = -2$ and $x_{ij} = 0$ for other i, j.

2.3. Full overlap case. We have *full overlap* between ϕ_1 and ϕ_2, if

$$(\Delta_1 x)^2 + (\Delta_2 x)^2 < |\sqrt{2\mu_1} - \sqrt{2\mu_2}|^2,$$

so that the disks of boundaries Σ_1^r and Σ_2^r are included one in the other, see Figure 3. In a highly interacting regime, this configuration leads to a *non-contractible* support for one of the two wave functions, which looses the symmetry properties of the trap. If the potentials are both centered at the origin, $\vartheta_{11} \gg \vartheta_{22}$, and the coupling ϑ_{12} is sufficiently large, as ϕ_2 spikes around the origin, ϕ_1 feels the influence of the coupling $\vartheta_{12}|\phi_j|^2\phi_i$, lowing down the profile (around the origin) and giving rise to a local minimum. This behaviour will be rigorously justified in the forthcoming section via energy estimates. In the Thomas–Fermi regime the location of the overlap regions depends upon the values of ϑ_{ij} and of the centers $\mathbf{x_i}$ according to formula (2.2). In order to visualize some situations arising with respect to the position of the trap

centers, see Figures 6 and 7 where we kept the ϑ_{ij}s fixed and varied the position of $\mathbf{x_1}$ ($x_{11} = \pm 2$ in Figure 6 and $x_{12} = \pm 2$ in Figure 7), while $\mathbf{x_2} = \mathbf{0}$.

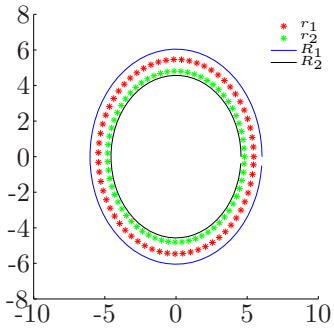

FIGURE 3. Supports of ϕ_1 and ϕ_2 (inside of starred disks) and disks related to the Thomas–Fermi approximation for ϕ_1 and ϕ_2 (overlap inside the smaller disk). We have taken $N_1 = N_2 = m_1 = m_2 = 1$, $\vartheta_{11} = 400$, $\vartheta_{22} = 200$, $\vartheta_{12} = 100$ and $x_{ij} = 0$ for other $i, j = 1, 2$.

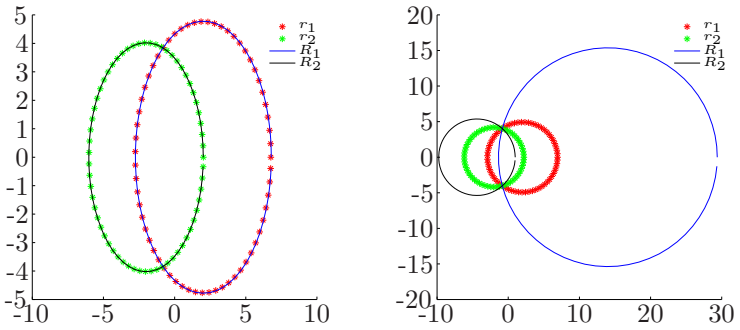

FIGURE 4. Supports of ϕ_1 and ϕ_2 (starred disks) and disks related to the Thomas–Fermi approximation for ϕ_1 and ϕ_2 (which holds within the intersection of the unstarred disks). We have taken $N_1 = N_2 = m_1 = m_2 = 1$, $\vartheta_{11} = 400$, $\vartheta_{22} = 200$, $\vartheta_{12} = 1$ (left figure) and $\vartheta_{12} = 150$ (right figure). In both figures we have $x_{11} = 2$, $x_{21} = -2$ and $x_{ij} = 0$ for other i, j.

3. Strong interaction and phase separation

In the next sections we deal with the justification of the phase separation phenomena occurring when the repulsive interaction between the condensates gets very strong. We consider both ground and excited state solutions. See also [**10**–**12**, **14**, **25**, **28**, **33**] for various studies of spatial segregation phenomena in systems with large interactions.

3.1. Ground state solutions. Assume that the intra-species parameters ϑ_{ii}s are chosen within a bounded range of values and, on the contrary, that the inter-species interaction rate ϑ_{12} becomes very large, say $\vartheta_{12} = \kappa$, where we let the parameter $\kappa \geq 0$ go to infinity. For notational simplicity, we set $\hbar = 1$. Let $\mathcal{H} \subset H^1(\mathbb{R}^2) \times H^1(\mathbb{R}^2)$ be the realization of the Hilbert subspace given in the introduction and consider the energy functional $E_\kappa : \mathcal{H} \to \mathbb{R}$ re-written as

$$E_\kappa(\phi_1, \phi_2) = E_\infty(\phi_1, \phi_2) + \kappa \int_{\mathbb{R}^2} |\phi_1|^2 |\phi_2|^2, \tag{3.1}$$

where

$$E_\infty(\phi_1, \phi_2) = \sum_{i=1}^{2} E_i(\phi_i).$$

Recalling (1.7), the energy level of the ground state solutions is

$$c_\kappa = \inf_{(\phi_1,\phi_2)\in\mathcal{S}} E_\kappa(\phi_1, \phi_2).$$

We also define the value for the limiting segregated least energy value c_∞,

$$c_\infty = \inf_{(\phi_1,\phi_2)\in\mathcal{S}_\infty} E_\infty(\phi_1, \phi_2),$$

where we have set

$$\mathcal{S}_\infty = \big\{(\phi_1, \phi_2) \in \mathcal{S} : \ \phi_1\phi_2 = 0 \text{ a.e. in } \mathbb{R}^2\big\}.$$

Proposition 3.1. *The sequence $(\phi_1^\kappa, \phi_2^\kappa) \subset \mathcal{S}$ of ground state solutions of* (1.5) *converges in $\mathcal{H}$ to a function $(\phi_1^\infty, \phi_2^\infty) \in \mathcal{S}_\infty$ at the energy level c_∞. Furthermore,*

$$-\frac{1}{2m_i}\Delta\phi_i^\infty + V_i(x_1, x_2)\phi_i^\infty + \vartheta_{ii}|\phi_i^\infty|^2\phi_i^\infty \leq \mu_i^\infty \phi_i^\infty, \tag{3.2}$$

where

$$N_i\mu_i^\infty = E_i(\phi_i^\infty) + \frac{\vartheta_{ii}}{2}\int_{\mathbb{R}^2} |\phi_i^\infty|^4,$$

for $i = 1, 2$.

Proof. The infimum that defines the value c_∞ is taken over a smaller set with respect to the one defining c_κ. Moreover, if the functions ϕ_1 and ϕ_2 have disjoint supports, $E_\kappa(\phi_1, \phi_2) = E_\infty(\phi_1, \phi_2)$, for any $\kappa > 0$. In particular, of course, this implies that $c_\kappa \leq c_\infty$, for all $\kappa > 0$. Therefore, for the ground state solutions $(\phi_1^\kappa, \phi_2^\kappa) \in \mathcal{H}$, $\phi_i^\kappa \not\equiv 0$ for $i = 1, 2$, we have $E_\kappa(\phi_1^\kappa, \phi_2^\kappa) = c_\kappa$ and

$$\kappa \int_{\mathbb{R}^2} |\phi_1^\kappa|^2 |\phi_2^\kappa|^2 \leq E_\infty(\phi_1^\kappa, \phi_2^\kappa) + \kappa \int_{\mathbb{R}^2} |\phi_1^\kappa|^2 |\phi_2^\kappa|^2 = c_\kappa \leq c_\infty, \tag{3.3}$$

for every $\kappa > 0$. As a consequence,

$$\lim_{\kappa\to\infty} \int_{\mathbb{R}^2} |\phi_1^\kappa|^2 |\phi_2^\kappa|^2 = 0. \tag{3.4}$$

Also, for all $\kappa > 0$, we have

$$\|(\phi_1^\kappa, \phi_2^\kappa)\|_{\mathcal{H}}^2 \leq E_\infty(\phi_1^\kappa, \phi_2^\kappa) + \kappa \int_{\mathbb{R}^2} |\phi_1^\kappa|^2 |\phi_2^\kappa|^2 \leq c_\infty,$$

so that the sequences $(\phi_1^\kappa, \phi_2^\kappa)$ is uniformly bounded in $\mathcal{H}$. In particular, up to a subsequence, there exist $(\phi_1^\infty, \phi_2^\infty)$ in $\mathcal{H}$ such that $(\phi_1^\kappa, \phi_2^\kappa) \rightharpoonup (\phi_1^\infty, \phi_2^\infty)$ in $\mathcal{H}$ as

$\kappa \to \infty$ and $\phi_i^\kappa(x_1,x_2) \to \phi_i^\infty(x_1,x_2)$ a.e. in $\mathbb{R}^2$. Hence, by combining Fatou's Lemma with formula (3.4), we get

$$\int_{\mathbb{R}^2} |\phi_1^\infty|^2 |\phi_2^\infty|^2 = 0,$$

so that

$$\phi_1^\infty \phi_2^\infty = 0, \quad \text{a.e. in } \mathbb{R}^2. \tag{3.5}$$

Since by definition of ground state solution $\int_{\mathbb{R}^2} |\phi_i^\kappa|^2 = N_i$, for any $\kappa > 0$, and $\mathcal{H}$ in compactly embedded into $L^2(\mathbb{R}^2) \times L^2(\mathbb{R}^2)$ (see inequality (3.8)), up to passing to a further subsequence, we conclude that

$$\int_{\mathbb{R}^2} |\phi_i^\infty|^2 = N_i, \tag{3.6}$$

for $i = 1, 2$. In particular $(\phi_1^\infty, \phi_2^\infty) \in \mathcal{S}_\infty$, by virtue of (3.5) and (3.6). Observe also that, by virtue of (1.6), (3.3) and $E_i(\phi_i^\kappa) \le c_\infty$,

$$\sup_{\kappa \ge 1} \mu_i^\kappa = \frac{1}{N_i} \sup_{\kappa \ge 1} \left\{ E_i(\phi_i^\kappa) + \frac{\vartheta_{ii}}{2} \int_{\mathbb{R}^2} |\phi_i^\kappa|^4 + \kappa \int_{\mathbb{R}^2} |\phi_1^\kappa|^2 |\phi_2^\kappa|^2 \right\} < \infty,$$

being μ_i^κ the eigenvalues corresponding to ϕ_i^κ. Then, up to a subsequence, $\mu_i^\kappa \to \mu_i^\infty$ as $\kappa \to \infty$. By testing the equations of (1.5) by an arbitrary positive function η with compact support, we get

$$\frac{1}{2m_i} \int_{\mathbb{R}^2} \nabla \phi_i^\kappa \cdot \nabla \eta + \int_{\mathbb{R}^2} V_i(x_1,x_2) \phi_i^\kappa \eta + \vartheta_{ii} \int_{\mathbb{R}^2} |\phi_i^\kappa|^2 \phi_i^\kappa \eta \le \mu_i^\kappa \int_{\mathbb{R}^2} \phi_i^\kappa \eta,$$

for all $\kappa > 0$ and any $\eta \in C_c^\infty(\mathbb{R}^2)$ with $\eta \ge 0$. Hence, letting $\kappa \to \infty$, it turns out that ϕ_i^∞ satisfies the variational inequality (3.2). Notice that, since $(\phi_1^\infty, \phi_2^\infty) \in \mathcal{S}_\infty$, by the definition of c_∞, we deduce

$$\begin{aligned}
&\sum_{i=1}^2 \frac{1}{2m_i} \int_{\mathbb{R}^2} |\nabla \phi_i^\infty|^2 + \sum_{i=1}^2 \int_{\mathbb{R}^2} V_i |\phi_i^\infty|^2 + \sum_{i=1}^2 \frac{\vartheta_{ii}}{2} \int_{\mathbb{R}^2} |\phi_i^\infty|^4 + \lim_{\kappa\to\infty} \kappa \int_{\mathbb{R}^2} |\phi_1^\kappa|^2 |\phi_2^\kappa|^2 \\
&\le \sum_{i=1}^2 \frac{1}{2m_i} \liminf_{\kappa\to\infty} \int_{\mathbb{R}^2} |\nabla \phi_i^\kappa|^2 + \sum_{i=1}^2 \liminf_{\kappa\to\infty} \int_{\mathbb{R}^2} V_i |\phi_i^\kappa|^2 + \sum_{i=1}^2 \frac{\vartheta_{ii}}{2} \liminf_{\kappa\to\infty} \int_{\mathbb{R}^2} |\phi_i^\kappa|^4 \\
&+ \lim_{\kappa\to\infty} \kappa \int_{\mathbb{R}^2} |\phi_1^\kappa|^2 |\phi_2^\kappa|^2 \le \liminf_{\kappa\to\infty} E_\kappa(\phi_1^\kappa, \phi_2^\kappa) = \liminf_{\kappa\to\infty} c_\kappa \le c_\infty \le E_\infty(\phi_1^\infty, \phi_2^\infty) \\
&= \sum_{i=1}^2 \frac{1}{2m_i} \int_{\mathbb{R}^2} |\nabla \phi_i^\infty|^2 + \sum_{i=1}^2 \int_{\mathbb{R}^2} V_i |\phi_i^\infty|^2 + \sum_{i=1}^2 \frac{\vartheta_{ii}}{2} \int_{\mathbb{R}^2} |\phi_i^\infty|^4,
\end{aligned}$$

which yields $\kappa \int_{\mathbb{R}^2} |\phi_1^\kappa|^2 |\phi_2^\kappa|^2 \to 0$ as $\kappa \to \infty$, which is a much stronger conclusion compared with (3.4). Consequently, the convergence of ϕ_i^κ to ϕ_i^∞ in $\mathcal{H}$ is strong, otherwise, assuming by contradiction that for some $i = 1, 2$

$$\int_{\mathbb{R}^2} |\nabla \phi_i^\infty|^2 < \lim_{\kappa\to\infty} \int_{\mathbb{R}^2} |\nabla \phi_i^\kappa|^2 \quad \text{or} \quad \int_{\mathbb{R}^2} V_i |\phi_i^\infty|^2 < \lim_{\kappa\to\infty} \int_{\mathbb{R}^2} V_i |\phi_i^\kappa|^2,$$

the previous inequalities we would become strict, yielding immediately a contradiction. Finally, as a further consequence, $c_\kappa \to c_\infty$ as $\kappa \to \infty$ and the value c_∞ is

indeed assumed and

$$c_\infty = \sum_{i=1}^{2} \frac{1}{2m_i} \int_{\mathbb{R}^2} |\nabla \phi_i^\infty|^2 + \sum_{i=1}^{2} \int_{\mathbb{R}^2} V_i |\phi_i^\infty|^2 + \sum_{i=1}^{2} \frac{\vartheta_{ii}}{2} \int_{\mathbb{R}^2} |\phi_i^\infty|^4 = E_\infty(\phi_1^\infty, \phi_2^\infty).$$

Finally, the strong convergence and (1.6) yield

$$N_i \mu_i^\infty = E_i(\phi_i^\infty) + \frac{\vartheta_{ii}}{2} \int_{\mathbb{R}^2} |\phi_i^\infty|^4$$

for any $i = 1, 2$, which concludes the proof. □

As we see in the numerical simulation, as the interaction coefficient gets large, the phase separation becomes rather evident. See the 2D contour plots of Figures 5, 6 and 7 where different choices of the centers of the potentials have been considered.

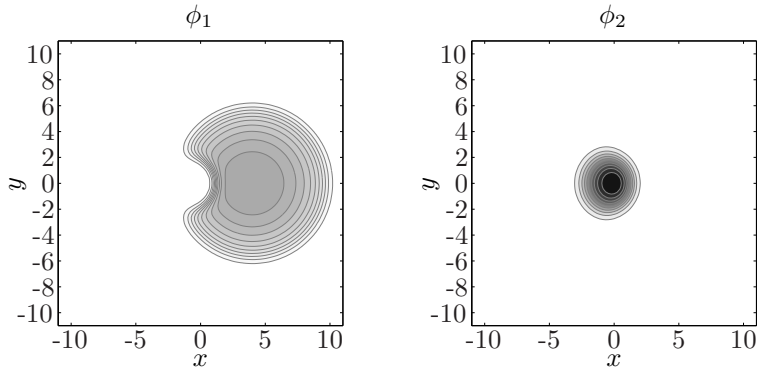

FIGURE 5. 2D contour plots, in the square $[-11, 11]^2$, of the ground state solution for $N_1 = N_2 = m_1 = m_2 = 1$, $\vartheta_{11} = 850$, $\vartheta_{22} = 18$, $\vartheta_{12} = 210$, where the potentials have centers $x_{11} = 4$ and $x_{ij} = 0$ for any other i, j. The phase separation is evident around the origin (partial overlap case).

3.2. The anisotropic case. Depending on the relative magnitude of parameters ω_{ij}, there are some directions along which the ground state solutions tends to concentrate. For instance, for ω_{11} (resp. ω_{12}) much larger than ω_{12} (resp. ω_{11}), the component ϕ_1 has a cigar-like shape along the y-axis (resp. x-axis). Similar behaviour for ϕ_2 along the y-axis (resp. x-axis) for ω_{21} (resp. ω_{22}) much larger than ω_{22} (resp. ω_{21}). In Figure 8 we consider the small interaction case, namely $\vartheta_{12} \ll \vartheta_{ii}$, when $\omega_{ii} = 100$ and $\omega_{ij} = 1$ for $i \neq j$. As it is evident from Figure 9, increasing the inter-specific coupling constant ($\vartheta_{12} = 1200$) the wave functions ϕ_1 and ϕ_2 spatially segregate around the origin.

3.3. Excited state solutions. As for the ground state solutions, in the strong interaction regime, also higher energy solutions exhibit a phase separation behaviour. These phenomena have also been confirmed by some numerical simulations, see e.g. the comparison in Figure 10 (top, $\vartheta_{12} = 0$ and bottom, $\vartheta_{12} = 120$) and in Figure 11 (top, $\vartheta_{12} = 0$ and bottom, $\vartheta_{12} = 120$). See also Section 4 for the notations.

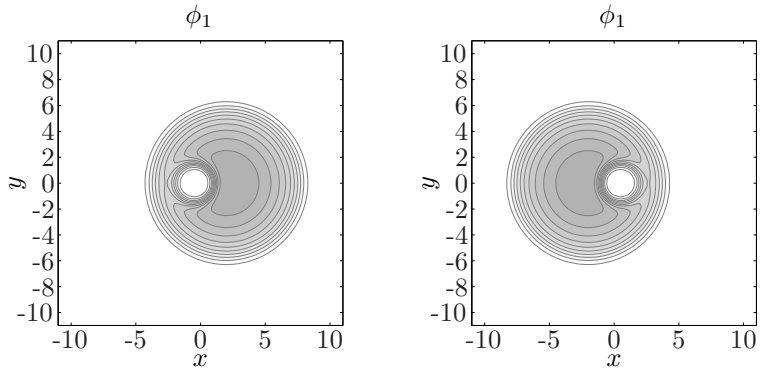

FIGURE 6. 2D contour plot, in the square $[-11, 11]^2$, of the first component of ground state solution for $N_1 = N_2 = m_1 = m_2 = 1$, $\vartheta_{11} = 850$, $\vartheta_{22} = 18$, $\vartheta_{12} = 210$ in the cases where the potentials have centers $x_{11} = 2$ and $x_{ij} = 0$ (left) and $x_{11} = -2$ and $x_{ij} = 0$ (right). The symmetry breaking is evident (full overlap case).

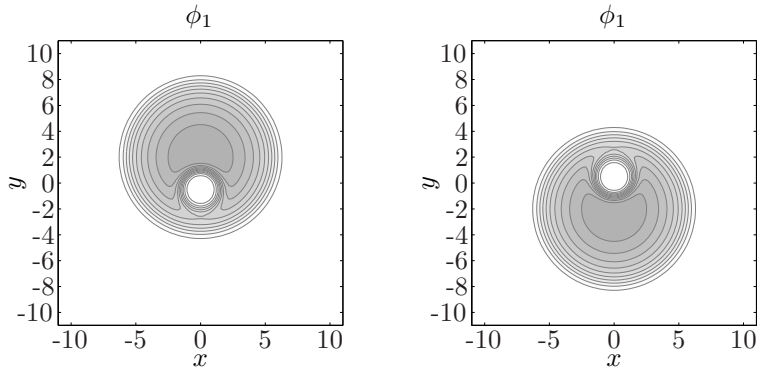

FIGURE 7. 2D contour plot, in the square $[-11, 11]^2$, of the first component of ground state solution for $N_1 = N_2 = m_1 = m_2 = 1$, $\vartheta_{11} = 850$, $\vartheta_{22} = 18$, $\vartheta_{12} = 210$ in the cases where the potentials have centers $x_{12} = 2$ and $x_{ij} = 0$ (left) and $x_{12} = -2$ and $x_{ij} = 0$ (right). The symmetry breaking is evident (full overlap case).

Consider the energy functional (3.1) defined on the space $\mathcal{H}$. If we consider the family of all subsets $A \subset \mathcal{H} \setminus \{(0,0)\}$ which are closed and symmetric w.r.t. the origin, the Krasnoselskii genus of $A \neq \emptyset$, denoted by $\gamma(A) \in \mathbb{N}$, is defined as the smallest positive integer n such that there exists an odd continuous function $\xi : A \to \mathbb{R}^n \setminus \{0\}$. We also set $\gamma(\emptyset) = 0$. When such an integer n fails to exist, we put $\gamma(A) = \infty$. Given a positive integer m, we can now introduce the families $\mathcal{E}$,

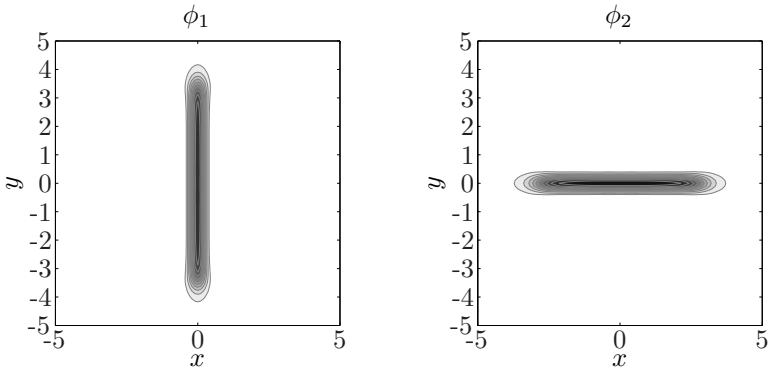

FIGURE 8. 2D contour plots, in the square $[-5,5]^2$, of the ground state solution for $N_1 = N_2 = m_1 = m_2 = 1$, $\vartheta_{11} = 400$, $\vartheta_{22} = 150$, $\vartheta_{12} = 1$, $\omega_{11} = 100$, $\omega_{22} = 100$, $\omega_{12} = \omega_{21} = 1$ and potentials centered at the origin.

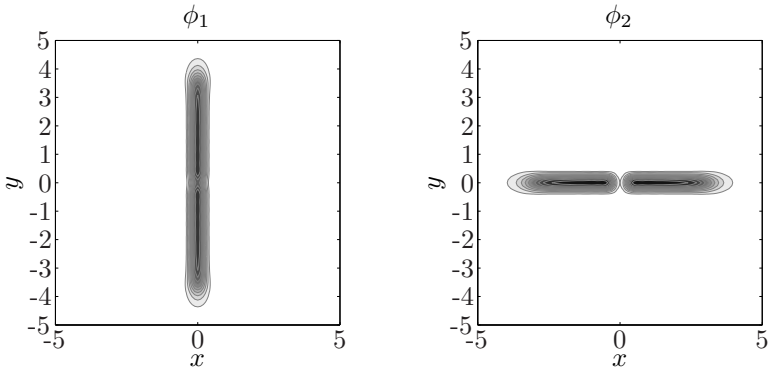

FIGURE 9. 2D contour plots, in the square $[-5,5]^2$, of the ground state solution for $N_1 = N_2 = m_1 = m_2 = 1$, $\vartheta_{11} = 400$, $\vartheta_{22} = 150$, $\vartheta_{12} = 1200$, $\omega_{11} = 100$, $\omega_{22} = 100$, $\omega_{12} = \omega_{21} = 1$ and potentials centered at the origin. The segregation around the origin is evident.

$\mathcal{E}_0$, Γ^m and Γ_0^m of subsets of $\mathcal{H}$, defined as follows:

$$\mathcal{E} = \big\{A \subset \mathcal{H} \setminus \{(0,0)\} : \ A \text{ is closed and symmetric w.r.t. the origin}\big\};$$

$$\mathcal{E}_0 = \big\{A \in \mathcal{E} : \text{ if } (\phi_1,\phi_2) \in A \text{ then } \phi_1\phi_2 = 0 \text{ a.e. in } \mathbb{R}^2\big\};$$

$$\Gamma^m = \big\{A \in \mathcal{E} : \ \gamma(A) \geq m \text{ and } \textstyle\int_{\mathbb{R}^2} \phi_1^2 = N_1, \ \int_{\mathbb{R}^2} \phi_2^2 = N_2 \text{ for any } (\phi_1,\phi_2) \in A\big\};$$

$$\Gamma_0^m = \big\{A \in \mathcal{E}_0 : \gamma(A) \geq m \text{ and } \textstyle\int_{\mathbb{R}^2} \phi_1^2 = N_1, \ \int_{\mathbb{R}^2} \phi_2^2 = N_2 \text{ for any } (\phi_1,\phi_2) \in A\big\}.$$

Then the candidates values to detect some critical (higher) levels of E_κ are

$$c_\kappa^m = \inf_{A \in \Gamma^m} \sup_{(\phi_1,\phi_2)\in A} E_\kappa(\phi_1,\phi_2).$$

We also introduce the following κ-independent values (notice that $E_\kappa|_{\mathcal{E}_0} = E_\infty$),

$$c_\infty^m = \inf_{A \in \Gamma_0^m} \sup_{(\phi_1,\phi_2)\in A} E_\infty(\phi_1,\phi_2).$$

Since $\mathcal{E}_0 \subset \mathcal{E}$, we have $\Gamma_0^m \subset \Gamma^m$ for any m and, then, by the above definitions,

$$c_\kappa^m \le c_\infty^m, \quad \text{for all } m \in \mathbb{N} \text{ and } \kappa > 0. \tag{3.7}$$

As we prove, the levels c_κ^m (which satisfy $c_\kappa^m \le c_\kappa^{m+1}$ as $\Gamma^{m+1} \subset \Gamma^m$ for any $m \in \mathbb{N}$) correspond to critical points of E_κ on $\mathcal{H}$ constrained to the sphere $\mathcal{S}$, thus yielding a sequence of nonlinear excited states of the Gross–Pitaevskii system (1.5).

PROPOSITION 3.2. *Let m a positive integer. Then, there exists a sequence of solutions $(\phi_1^{\kappa,m}, \phi_2^{\kappa,m})$ of system (1.5) at energy levels c_κ^m such that, in the large competition limit $\kappa \to \infty$, it converges, weakly in $\mathcal{H}$ and strongly in $L^q(\mathbb{R}^2)$ for any $q \ge 2$ to a limit configuration $(\phi_1^{\infty,m}, \phi_2^{\infty,m}) \in \mathcal{S}_\infty$.*

REMARK 3.3. Contrary to the case of ground state solutions it seems not possible to show that the limiting configuration $(\phi_1^{\infty,m}, \phi_2^{\infty,m})$ corresponds to the energy level c_∞^m for the functional E_∞ and satisfies suitable variational inequalities.

In order to prove Proposition 3.2, we first show that, since $V_i \to \infty$ for $(x_1, x_2) \to \infty$, E_κ satisfies a technical compactness condition, the Palais–Smale condition. For the sake of completeness, we shall include a proof of this fact.

LEMMA 3.4. *For any $\kappa > 0$ the functional $E_\kappa|_{\mathcal{S}}$ satisfies the Palais–Smale condition, namely for any sequence (ϕ_n^1, ϕ_n^2) in $\mathcal{S}$ such that $E_\kappa(\phi_n^1, \phi_n^2)$ is bounded and $dE_\kappa|_{\mathcal{S}}(\phi_n^1, \phi_n^2) \to 0$ as $n \to \infty$ in the dual space $\mathcal{H}^*$ of $\mathcal{H}$ (called Palais–Smale sequence) there exists a strongly convergent subsequence in $\mathcal{H}$.*

PROOF. Let $\kappa > 0$ and let $(\phi_n^1, \phi_n^2) \subset \mathcal{S}$ be a Palais–Smale sequence for E_κ. In particular,

$$\sup_{n\ge1} \|(\phi_n^1, \phi_n^2)\|_{\mathcal{H}}^2 \le \sup_{n\ge1} E_\kappa(\phi_n^1, \phi_n^2) < \infty$$

Hence (ϕ_n^1, ϕ_n^2) is bounded in $\mathcal{H}$ and, up to a subsequence, it converges weakly in $\mathcal{H}$, and for a.e. (x_1, x_2) in $\mathbb{R}^2$, to a function $(\phi_\infty^1, \phi_\infty^2) \in \mathcal{H}$. Notice that $\mathcal{H}$ is compactly embedded into $L^2(\mathbb{R}^2) \times L^2(\mathbb{R}^2)$ as for any $i = 1, 2$ and for any $R > 0$, we have

$$\sup_{n\ge1} R^2 \int_{\mathbb{R}^2 \setminus B_R(x_{i1}, x_{i2})} (\phi_n^i)^2 < \infty. \tag{3.8}$$

Then, up to a further subsequence, $\phi_n^i \to \phi_\infty^i$ in $L^2(\mathbb{R}^2)$ as $n \to \infty$, which yields $(\phi_\infty^1, \phi_\infty^2) \in \mathcal{S}$. Hence, by the Gagliardo–Nirenberg interpolation inequality

$$\|\phi\|_{L^{\frac{2}{1-\alpha}}(\mathbb{R}^2)} \le c\|\nabla\phi\|_{L^2(\mathbb{R}^2)}^{\alpha} \|\phi\|_{L^2(\mathbb{R}^2)}^{1-\alpha}, \qquad \forall \alpha \in [0,1),\ \forall \phi \in H^1(\mathbb{R}^2), \tag{3.9}$$

taking, in particular, $\alpha = 1/2$ we get ($c > 0$ changes from inequality to inequality)

$$\|\phi_n^i - \phi_\infty^i\|_{L^4(\mathbb{R}^2)} \le c\|\nabla\phi_n^i - \nabla\phi_\infty^i\|_{L^2(\mathbb{R}^2)}^{1/2} \|\phi_n^i - \phi_\infty^i\|_{L^2(\mathbb{R}^2)}^{1/2} \le c\|\phi_n^i - \phi_\infty^i\|_{L^2(\mathbb{R}^2)}^{1/2}$$

so that ϕ_n^i converges to ϕ_∞^i strongly in $L^4(\mathbb{R}^2)$ as $n \to \infty$ (actually in any L^q), for $i = 1, 2$. Now, by virtue of the condition $dE_\kappa|_{\mathcal{S}}(\phi_n^1, \phi_n^2) \to 0$ as $n \to \infty$, there exists a sequence (w_n) in $\mathcal{H}^*$ with $w_n \to 0$ in $\mathcal{H}^*$ as $n \to \infty$ and two sequences $(\mu_n^i) \subset \mathbb{R}$,

$i=1,2$, such that, for all $(\varphi,\eta)\in\mathcal{H}$,

$$\frac{1}{2m_1}\int_{\mathbb{R}^2}\nabla\phi_n^1\cdot\nabla\varphi+\int_{\mathbb{R}^2}V_1(x_1,x_2)\phi_n^1\varphi+\vartheta_{11}\int_{\mathbb{R}^2}|\phi_n^1|^2\phi_n^1\varphi+\kappa\int_{\mathbb{R}^2}|\phi_n^2|^2\phi_n^1\varphi$$

$$+\frac{1}{2m_2}\int_{\mathbb{R}^2}\nabla\phi_n^2\cdot\nabla\eta+\int_{\mathbb{R}^2}V_2(x_1,x_2)\phi_n^2\eta+\kappa\int_{\mathbb{R}^2}|\phi_n^1|^2\phi_n^2\eta+\vartheta_{22}\int_{\mathbb{R}^2}|\phi_n^2|^2\phi_n^2\eta$$

$$=\mu_n^1\int_{\mathbb{R}^2}\phi_n^1\varphi+\mu_n^2\int_{\mathbb{R}^2}\phi_n^2\eta+\langle w_n,(\varphi,\eta)\rangle \tag{3.10}$$

Observe that, by choosing $\varphi=\phi_n^1$ and $\eta=0$ (resp. $\varphi=0$ and $\eta=\phi_n^2$) and recalling that $\int_{\mathbb{R}^2}(\phi_n^i)^2=N_i$, we get a representation formula for μ_n^1 (resp. μ_n^2). It follows that (μ_n^i) is bounded in $\mathbb{R}$ so that, up to a subsequence, it converges to some positive number μ_∞^i. Finally, choosing any arbitrary $(\varphi,0)\in\mathcal{H}$ and $(0,\eta)\in\mathcal{H}$ as test functions in the previous identity and taking the limit as $n\to\infty$, it holds

$$\frac{1}{2m_1}\int_{\mathbb{R}^2}\nabla\phi_\infty^1\cdot\nabla\varphi+\int_{\mathbb{R}^2}V_1(x_1,x_2)\phi_\infty^1\varphi+\vartheta_{11}\int_{\mathbb{R}^2}|\phi_\infty^1|^2\phi_\infty^1\varphi$$
$$+\kappa\int_{\mathbb{R}^2}|\phi_\infty^2|^2\phi_\infty^1\varphi=\mu_\infty^1\int_{\mathbb{R}^2}\phi_\infty^1\varphi, \tag{3.11}$$

$$\frac{1}{2m_2}\int_{\mathbb{R}^2}\nabla\phi_\infty^2\cdot\nabla\eta+\int_{\mathbb{R}^2}V_2(x_1,x_2)\phi_\infty^2\eta+\kappa\int_{\mathbb{R}^2}|\phi_\infty^1|^2\phi_\infty^2\eta$$
$$+\vartheta_{22}\int_{\mathbb{R}^2}|\phi_\infty^2|^2\phi_\infty^2\eta=\mu_\infty^2\int_{\mathbb{R}^2}\phi_\infty^2\eta. \tag{3.12}$$

In particular $(\phi_\infty^1,\phi_\infty^2)\in\mathcal{H}$ is a weak solution of

$$\begin{cases}-\frac{1}{2m_1}\Delta\phi_\infty^1+V_1(x_1,x_2)\phi_\infty^1+\vartheta_{11}|\phi_\infty^1|^2\phi_\infty^1+\kappa|\phi_\infty^2|^2\phi_\infty^1=\mu_\infty^1\phi_\infty^1,\\ -\frac{1}{2m_2}\Delta\phi_\infty^2+V_2(x_1,x_2)\phi_\infty^2+\kappa|\phi_\infty^1|^2\phi_\infty^2+\vartheta_{22}|\phi_\infty^2|^2\phi_\infty^2=\mu_\infty^2\phi_\infty^2.\end{cases}$$

Now, choosing $\varphi=\phi_n^1$ and $\eta=\phi_n^2$ in (3.10), $\varphi=\phi_\infty^1$ in (3.11) and $\eta=\phi_\infty^2$ in (3.12), taking into account the strong convergence of ϕ_n^i to ϕ_∞^i in $L^4(\mathbb{R}^2)$, that (ϕ_n^1,ϕ_n^2) is bounded in $\mathcal{H}$ and $w_n\to0$ in $\mathcal{H}^*$, by the resulting identities we get

$$\lim_{n\to\infty}\|(\phi_n^1,\phi_n^2)\|_{\mathcal{H}}^2=\lim_{n\to\infty}\sum_{i=1}^2\frac{1}{2m_i}\int_{\mathbb{R}^2}|\nabla\phi_n^i|^2+\int_{\mathbb{R}^2}V_i(x_1,x_2)(\phi_n^i)^2$$

$$=\lim_{n\to\infty}\Big[N_1\mu_n^1+N_2\mu_n^2-\sum_{i=1}^2\vartheta_{ii}\int_{\mathbb{R}^2}|\phi_n^i|^4-2\kappa\int_{\mathbb{R}^2}|\phi_n^1|^2|\phi_n^2|^2+\langle w_n,(\phi_n^1,\phi_n^2)\rangle\Big]$$

$$=N_1\mu_\infty^1+N_2\mu_\infty^2-\sum_{i=1}^2\vartheta_{ii}\int_{\mathbb{R}^2}|\phi_\infty^i|^4-2\kappa\int_{\mathbb{R}^2}|\phi_\infty^1|^2|\phi_\infty^2|^2$$

$$=\sum_{i=1}^2\frac{1}{2m_i}\int_{\mathbb{R}^2}|\nabla\phi_\infty^i|^2+\int_{\mathbb{R}^2}V_i(x_1,x_2)(\phi_\infty^i)^2=\|(\phi_\infty^1,\phi_\infty^2)\|_{\mathcal{H}}^2,$$

where we used the fact that $\phi_n^1\phi_n^2\to\phi_\infty^1\phi_\infty^2$ in $L^2(\mathbb{R}^2)$, following by

$$\int_{\mathbb{R}^2}|\phi_n^1\phi_n^2-\phi_\infty^1\phi_\infty^2|^2\le2\|\phi_n^1\|_{L^4(\mathbb{R}^2)}^2\|\phi_n^2-\phi_\infty^2\|_{L^4(\mathbb{R}^2)}^2+2\|\phi_\infty^2\|_{L^4(\mathbb{R}^2)}^2\|\phi_n^1-\phi_\infty^1\|_{L^4(\mathbb{R}^2)}^2.$$

Hence (ϕ_n^1,ϕ_n^2) converges in $\mathcal{H}$, proving the Palais–Smale condition. □

We now recall the following existence result (see e.g. [**34**, Theorem 5.7]).

Let $(X, \|\cdot\|)$ be a infinite dimensional Banach space and let $Y \subset X \setminus \{0\}$ be a complete symmetric $C^{1,1}$-manifold. Let $f : Y \to \mathbb{R}$ be an even functional of class C^1. Assume that f satisfies the Palais–Smale condition and is bounded from below on Y. Then f admits at least $N = \sup\{\gamma(K) : K \subset Y \text{ compact and symmetric}\}$ critical points.

We are now ready to prove Proposition 3.2.

Proof of Proposition 3.2. Since E_κ is a C^1 functional, satisfies the Palais–Smale condition by Lemma 3.4, is even and bounded from below (as $E_\kappa \geq 0$), the above mentioned result applies with $Y = \mathcal{S}$ yielding (it holds $N = \infty$) a sequence of solutions $(\phi_1^{\kappa,m}, \phi_2^{\kappa,m})$ in $\mathcal{S}$ to (1.5) with $E_\kappa(\phi_1^{\kappa,m}, \phi_2^{\kappa,m}) = c_\kappa^m$, $m \geq 1$ and $\kappa > 0$. With reference to (3.1), by means of (3.7) this implies that

$$\kappa \int_{\mathbb{R}^2} |\phi_1^{\kappa,m}|^2 |\phi_2^{\kappa,m}|^2 \leq E_\infty(\phi_1^{\kappa,m}, \phi_2^{\kappa,m}) + \kappa \int_{\mathbb{R}^2} |\phi_1^{\kappa,m}|^2 |\phi_2^{\kappa,m}|^2 = c_\kappa^m \leq c_\infty^m,$$

for every $\kappa > 0$. As a consequence, as c_∞^m is independent of κ, for any $m \geq 1$,

$$\lim_{\kappa \to \infty} \int_{\mathbb{R}^2} |\phi_1^{\kappa,m}|^2 |\phi_2^{\kappa,m}|^2 = 0. \tag{3.13}$$

Similarly, as $\|(\phi_1^{\kappa,m}, \phi_2^{\kappa,m})\|_{\mathcal{H}}^2 \leq c_\kappa^m \leq c_\infty^m$, it follows that $(\phi_1^{\kappa,m}, \phi_2^{\kappa,m})_{\kappa>0}$ is bounded in $\mathcal{H}$. Hence, up to a subsequence, $(\phi_1^{\kappa,m}, \phi_2^{\kappa,m})_{\kappa>0}$ weakly converges in $\mathcal{H}$ (and strongly in $L^q(\mathbb{R}^2)$ for any $q \geq 2$, by combining formulas (3.8)-(3.9)) to a function $(\phi_1^{\infty,m}, \phi_2^{\infty,m}) \in \mathcal{H}$. In particular,

$$\int_{\mathbb{R}^2} |\phi_i^{\infty,m}|^2 = N_i \quad \text{and} \quad \phi_1^{\infty,m} \phi_2^{\infty,m} = 0 \quad \text{a.e. in } \mathbb{R}^2,$$

which proves the assertion. □

4. Numerical computation of solutions

We describe the numerical algorithm used for the computation of the ground states for the single one-dimensional Gross–Pitaevskii equation and we mention at the end of this section how the same technique can be applied to a system of any number of coupled equations in $\mathbb{R}^2$. Moreover, without loss of generality, we reduce to the case $\hbar = m = 1$. The main idea is to directly minimize the energy $E(\phi)$ associated to a wave function $\psi(x) = e^{-i\mu t}\phi(x)$, discretized by Hermite functions. As it is known, the Hermite functions $(\mathcal{H}_l^\beta)_{l\in\mathbb{N}}$ are defined by

$$\mathcal{H}_l^\beta(x) = H_l^\beta(x) e^{-\frac{1}{2}\beta^2 x^2}, \quad l \in \mathbb{N},$$

where $(H_l^\beta)_{l\in\mathbb{N}}$ are the *Hermite polynomials* [**7**], orthonormal in L^2 with respect to the weight $e^{-\beta^2 x^2}$. The Hermite functions are the solutions (ground state, for $l = 0$, and excited states, if else) to the eigenvalue problem for the linear Schrödinger equation with standard harmonic potential

$$\frac{1}{2}\left(-\frac{d^2}{dx^2} + (\beta^2 x)^2\right)\mathcal{H}_l = \lambda_l \mathcal{H}_l, \qquad \lambda_l = \beta^2\left(l + \frac{1}{2}\right).$$

If we set

$$\phi = \sum_{l\in\mathbb{N}} \phi_l \mathcal{H}_l,$$

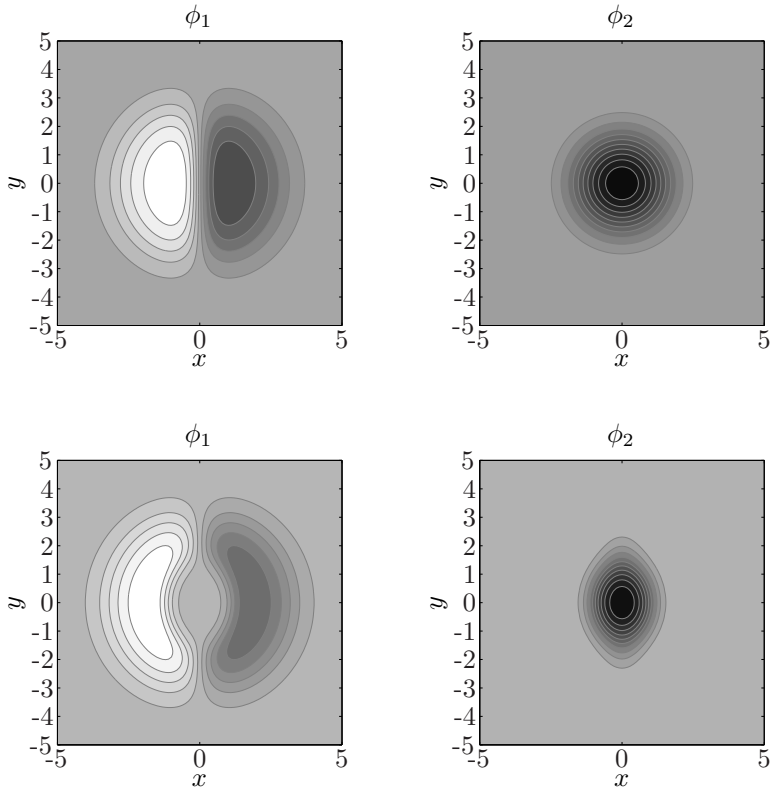

FIGURE 10. 2D contour plots, in the square $[-5,5]^2$, of an excited state solution of the system. In the left figures (two nodal regions) we have the ϕ_1 component corresponding to $N_1 = N_2 = m_1 = m_2 = 1$, $l_1 = 1$, $l_2 = 0$ (initial guess), $\vartheta_{11} = 50$, $\vartheta_{22} = 5$, $\vartheta_{12} = 0$ (top) and $\vartheta_{12} = 120$ (bottom). In the right figures (no nodal regions) we have the corresponding ϕ_2 component, with $l_1 = l_2 = 0$ (initial guess). The potentials are centered at the origin.

where

$$\phi_l = (\phi, \mathcal{H}_l)_{L^2} = \int_{\mathbb{R}} \phi \mathcal{H}_l,$$

the energy functional rewrites as

$$E(\phi) = \sum_{l\in\mathbb{N}} \lambda_l \phi_l^2 + \int_{\mathbb{R}} \left(V(x) - \frac{(\beta^2 x)^2}{2} \right) \left(\sum_{l\in\mathbb{N}} \phi_l \mathcal{H}_l \right)^2 + \frac{1}{2}\vartheta \int_{\mathbb{R}} \left(\sum_{l\in\mathbb{N}} \phi_l \mathcal{H}_l \right)^4,$$

and the chemical potential turns into

$$N\mu = E(\phi) + \frac{1}{2}\vartheta \int_{\mathbb{R}} \left(\sum_{l\in\mathbb{N}} \phi_l \mathcal{H}_l \right)^4 \tag{4.1}$$

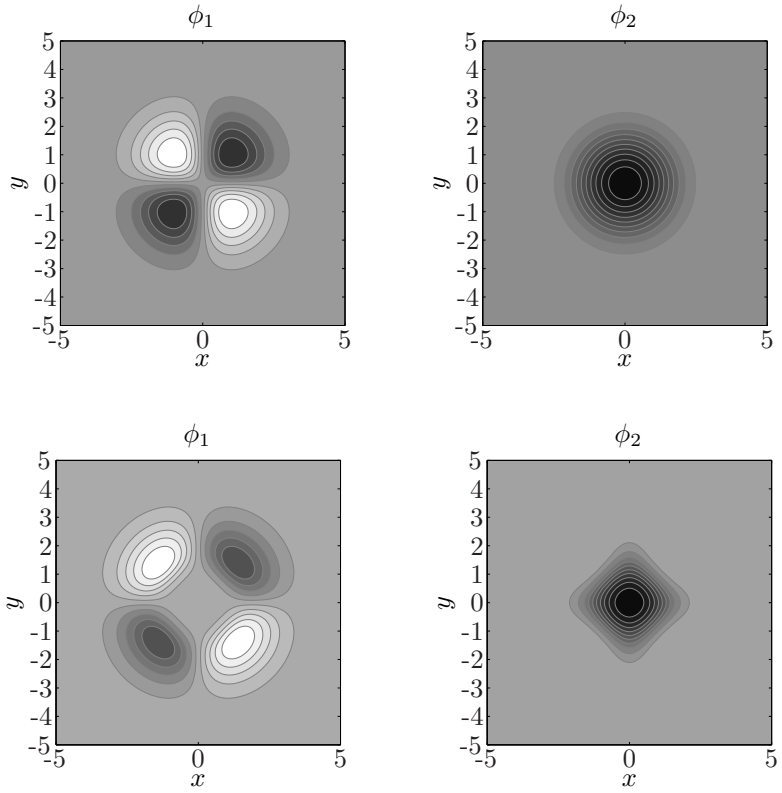

FIGURE 11. 2D contour plots, in the square $[-5,5]^2$, of an excited state solution of the system. In the left figures (four nodal regions) we have the ϕ_1 component corresponding to $N_1 = N_2 = m_1 = m_2 = 1$, $l_1 = l_2 = 1$ (initial guess), $\vartheta_{11} = 10$, $\vartheta_{22} = 5$, $\vartheta_{12} = 0$ (top) and $\vartheta_{12} = 120$ (bottom). In the right figures (no nodal regions) we have the corresponding ϕ_2 component, with $l_1 = l_2 = 0$ (initial guess). The potentials are centered at the origin. Visibly, the supports of the ϕ_is segregate around the origin.

By minimizing E, under the constraint $\|\phi\|_{L^2}^2 = N$, we look for local minima of

$$E(\phi;\lambda) = E(\phi) + \lambda\left(N - \sum_{l\in\mathbb{N}} \phi_l^2\right)$$

which solve the system, with $k \in \mathbb{N}$,

$$\begin{cases} (\lambda_\kappa - \lambda)\phi_\kappa + \displaystyle\int_{\mathbb{R}} \left(V(x) - \frac{(\beta^2 x)^2}{2}\right) \mathcal{H}_k \left(\sum_{l\in\mathbb{N}} \phi_l \mathcal{H}_l\right) + \vartheta \int_{\mathbb{R}} \mathcal{H}_k \left(\sum_{l\in\mathbb{N}} \phi_l \mathcal{H}_l\right)^3 = 0, \\ \displaystyle\sum_{l\in\mathbb{N}} \phi_l^2 = N. \end{cases}$$

We notice that, if ϕ is a solution of the above system, then it is immediately seen, by multiplying times ϕ_k, summing up over k and using (4.1), that the Lagrange multiplier λ equals the chemical potential μ. Next, we truncate to degree $L-1$ and

introduce an additional parameter $\rho = 1$ in front of the first integral (its usage will be clear later), to obtain a corresponding truncated energy functional $E_L(\phi; \lambda; \rho)$, whose local minima solve the system, with $0 \le k \le L-1$,

$$\begin{cases} (\lambda_\kappa - \lambda)\phi_\kappa + \rho \displaystyle\int_{\mathbb{R}} \left(V(x) - \frac{(\beta^2 x)^2}{2} \right) \mathcal{H}_k \left(\sum_{l=0}^{L-1} \phi_l \mathcal{H}_l \right) + \vartheta \int_{\mathbb{R}} \mathcal{H}_k \left(\sum_{l=0}^{L-1} \phi_l \mathcal{H}_l \right)^3 = 0, \\ \displaystyle\sum_{l=0}^{L-1} \phi_l^2 = N. \end{cases}$$

In order to approximate the integrals, we used a Gauss–Hermite quadrature formula with $2L-1$ nodes relative to the weight $e^{-2\beta^2 x^2}$. Using the tensor basis of the Hermite functions, i.e.

$$\mathcal{H}_l(x_1, x_2) = H_{l_1}^{\beta_1}(x_1) H_{l_2}^{\beta_2}(x_2) e^{-\frac{1}{2}(\beta_1^2 x_1^2 + \beta_2^2 x_2^2)}$$

the extension to the two-dimensional case is straightforward. In particular, in $\mathbb{R}^2$, $\mathcal{H}_{0,0}(x_1, x_2)$ is the ground eigenstate and $\mathcal{H}_{l_1,l_2}(x_1, x_2)$ with any $l_1 \neq 0$ or $l_2 \neq 0$ is an excited eigenstate of the Schrödinger equation with standard harmonic potential. See Figures 12 and 13 representing $\mathcal{H}_{1,0}$, $\mathcal{H}_{1,1}$, $\mathcal{H}_{2,1}$ and $\mathcal{H}_{2,2}$. For small coupling constants excited states solutions of the GPE system look like these profiles, see e.g. Figures 10 and 11. The extension to a system of any number of equations is not difficult, too. In fact, it is sufficient to consider the total energy of the system as the functional to be minimized, with a normalization constraint (Lagrange multiplier) for each wave function.

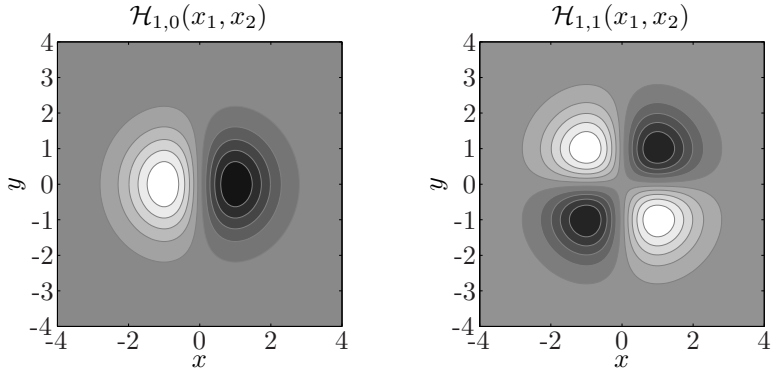

FIGURE 12. 2D contour plots of Hermite functions with $l_1 = 1$, $l_2 = 0$, $\beta_1 = \beta_2 = 1$ (left picture, one nodal region) and $l_1 = l_2 = 1$, $\beta_1 = \beta_2 = 1$ (right picture, two nodal regions).

The system is solved by a modified Newton method with backtracking line-search, which guarantees global convergence to the ground states. We refer to [**6**, **9**] and, in particular, to [**8**] for the details. Here we just mention that only the diagonal part of the Jacobian relative to ϕ_l is computed, thus leading to a dramatic reduction of the computational cost for the solution of each linear system. Moreover, the initial guess for the Newton iteration is obtained by a continuation technique over ρ and ϑ, starting from the ground state of the Schrödinger equation with the standard harmonic potential, which corresponds to $\rho = \vartheta = 0$. The convergence to the excited states is not guaranteed, although we observed numerical convergence for

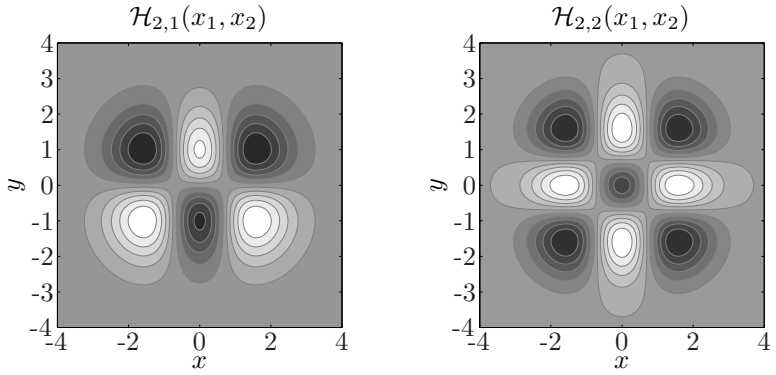

FIGURE 13. 2D contour plots of Hermite functions with $l_1 = 2$, $l_2 = 1$, $\beta_1 = \beta_2 = 1$ (left picture, three nodal regions) and $l_1 = l_2 = 2$, $\beta_1 = \beta_2 = 1$ (right picture, four nodal regions).

the examples reported in the previous section. Of course the case of very large values of the coefficients ϑ_{ij} can be treated within the framework of the Thomas–Fermi approximation.

Acknowledgments

The authors wish to thank Prof. Mark Ablowitz for providing some useful bibliographic references.

References

1. M.J. Ablowitz, B. Prinari, A.D. Trubatch, *Discrete and continuous nonlinear Schrödinger systems*, London Mathematical Society, Lecture Note Series, 302. Cambridge University Press, Cambridge, 2004.
2. M.J. Ablowitz, B. Prinari, A.D. Trubatch, *Integrable nonlinear Schrödinger systems and their soliton dynamics*, Dyn. Partial Differ. Equ. **1** (2004), 239–301.
3. M.J. Ablowitz, B. Prinari, A.D. Trubatch, *Soliton interactions in the vector NLS equation*, Inverse Problems **20** (2004), 1217–1237.
4. M.H. Anderson, J.R. Ensher, M.R. Matthews, C.E. Wieman, E.A. Cornell, *Observation of Bose–Einstein condensation in a diluite atomic vapor*, Science **269** (1995), 198–201.
5. W. Bao, *Ground states and dynamics of multicomponent Bose–Einstein condensates*, Multiscale Model. Simul. **2** (2004), 210–236.
6. W. Bao, W. Tang, *Ground-state solution of Bose–Einstein condensate by directly minimizing the energy functional*, J. Comp. Phys. **187** (2003), 230–254.
7. J.P. Boyd, *Chebyshev and Fourier spectral methods*, Dover, New York, 2001.
8. M. Caliari, A. Ostermann, S. Rainer, M. Thalhammer, *A minimisation approach for computing the ground state of Gross–Pitaevskii systems*, preprint, (2008).
9. M. Caliari, M. Thalhammer, *High-order time-splitting Fourier–Hermite spectral methods for the Gross–Pitaevskii equation*, preprint, (2007).
10. M. Conti, S. Terracini, G. Verzini, *Nehari's problem and competing species systems*, Ann. Inst. H. Poincaré Anal. Non Linéaire **19** (2002), 871–888.
11. E.C.M. Crooks, E.N. Dancer, D. Hilhorst, *On long-time dynamics for competition-diffusion systems with inhomogeneous Dirichlet boundary conditions*, Topol. Meth. Nonlin. Anal. **30** (2007), 1–36.
12. E.C.M. Crooks, E.N. Dancer, D. Hilhorst, M. Mimura, H. Ninomiya, *Spatial segregation limit for a competition-diffusion system with Dirichlet boundary conditions*, Nonlinear Anal. Real World Appl. **5** (2004), 645–665.

13. F. Dalfovo, S. Giorgini, L.P. Pitaevskii, S. Stringari, *Theory of trapped Bose–condensed gases*, Rev. Mod. Phys. **71** (1999), 463–512.
14. E.N. Dancer, Z. Zhang, *Dynamics of Lotka–Volterra competition systems with large interactions*, J. Differential Equations **182** (2002), 470–489.
15. B.D. Esry, C.H. Greene, J.P.. Burke, J.L. Bohn, *Hartree–Fock theory for double condensates*, Phys. Rev. Lett. **78** (1997), 3594–3597.
16. E. Fermi, Rend. Lincei **6**, (1927), 602–607.
17. E.P. Gross, *Structure of a quantized vortex in boson systems*, Nuovo Cimento **20** (1961), 454–477.
18. A.G. Kalocsai, J.W. Haus, *Asymptotic wave-wave processes beyond cascading in quadratic nonlinear optical materials*, Phys. Rev. E **52** (1995), 3166–3183.
19. N. Lazarides, G.P. Tsironis, *Coupled nonlinear Schrödinger field equations for electromagnetic wave propagation in nonlinear left-handed materials*, Phys. Rev. E **71**, 036614 (2005).
20. E.H. Lieb, *Thomas–Fermi and related theories of atoms and molecules*, Rev. Mod. Phys. **53** (1981), 603–641.
21. E.H. Lieb, B. Simon, *Thomas–Fermi theory revisited*, Phys. Rev. Lett. **31** (1973), 681–683.
22. U. Lindner, V. Fedyanin, *Solitons in a one-dimensional modified Hubbard model*, Phys. Status Solidi B **89** (1978), 123–129.
23. V.G. Makhankov, *Quasi-classical solitons in the Lindner–Fedyanin model hole-like excitations*, Phys. Lett. A **81** (1981), 156–160.
24. C.R. Menyuk, *Nonlinear pulse propagation in birefringent optical fibers*, IEEE J. Quantum Electron. **23** (1987), 174–176.
25. M. Mimura, K. Kawasaki, *Spatial segregation in competitive interaction-diffusion equations*, J. Math. Biol. **9** (1980), 49–64.
26. C.J. Myatt, E.A. Burt, R.W. Ghrist, E.A. Cornell, C.E. Wieman, *Production of two overlapping Bose–Einstein condensates by sympathetic cooling*, Phys. Rev. Lett. **78** (1997), 586–589.
27. E. Montefusco, B. Pellacci, M. Squassina, *Semiclassical states for weakly coupled nonlinear Schrödinger systems*, J. Eur. Math. Soc. (JEMS) **10** (2008), 47–71.
28. T. Namba, M. Mimura, *Spatial distribution for competing populations*, J. Theoret. Biol. **87** (1980), 795–814.
29. L.P. Pitaevskii, *Vortex lines in an imperfect Bose gas*, Sov. Phys. JETP **13** (1961), 451–454.
30. L.P. Pitaevskii, S. Stringari, *Bose–Einstein condensation*, Oxford Science Publications, Int. Series of Monographs on Physics, 2003.
31. P.H. Rabinowitz, *Minimax methods in critical point theory with applications to differential equations*, AMS Monograph, **65** (1986).
32. F. Riboli, M. Modugno, *Topology of the ground state of two interacting Bose–Einstein condensates*, Phys. Rev. A **65** 063614 (2002).
33. M. Squassina, *On the long term spatial segregation for a competition-diffusion system*, Asymptotic Anal., to appear, (2008).
34. M. Struwe, *Variational methods*, third edition, Springer (2000).
35. L.H. Thomas, *The calculation of atomic fields*, Proc. Cambridge Phil. Soc. **23** (1927), 542–548.
36. E. Timmermans, *Phase separation of Bose–Einstein condensates*, Phys. Rev. Lett. **81** (1998), 5718–5721.

Current address: Dipartimento di Informatica, Università di Verona, Cà Vignal 2, Strada Le Grazie 15, I-37134 Verona, Italy.
E-mail address: marco.caliari@univr.it

Current address: Dipartimento di Informatica, Università di Verona, Cà Vignal 2, Strada Le Grazie 15, I-37134 Verona, Italy.
E-mail address: marco.squassina@univr.it